Mechatronics 21 (2011) 250–260

Contents lists available at ScienceDirect

Mechatronics

journal homepage: www.elsevier.com/locate/mechatronics

Vibration control for active seat suspension systems via dynamic output feedback with limited frequency characteristic

Weichao Sun, Jinfu Li, Ye Zhao, Huijun Gao *

Space Control and Inertial Technology Research Center, Harbin Institute of Technology, Harbin, China

ARTICLE INFO

Article history:
Received 11 June 2010
Accepted 2 November 2010
Available online 30 November 2010

Keywords:
Active seat suspension systems
Dynamic output feedback
Finite frequency
H_∞ control

ABSTRACT

This paper investigates the problem of H_∞ control for active seat suspension systems via dynamic output feedback control. A vertical vibration model of human body is introduced in order to make the modeling of seat suspension systems more precise. Meantime, different from the existing H_∞ control methods which conduct disturbance attenuation within the entire frequency domain, this paper addresses the problem of H_∞ control for active seat suspension systems in finite frequency domain to match the characteristics of the human body. By using the generalized Kalman–Yakubovich–Popov (KYP) lemma, the H_∞ norm from the disturbance to the controlled output is decreased over the chosen frequency band between which the human body is extremely sensitive to the vibration, to improve the ride comfort. Considering a practical situation of active seat suspension systems, a dynamic output feedback controller of order equal to the plant is designed, where an effective multiplier expansion is used to convert the controller design to a convex optimization problem. Compared with the entire frequency approach for active seat suspension systems, the finite frequency approach achieves better disturbance attenuation for the concerned frequency range, while the performance constraint is guaranteed in the controller design, which is verified by a practical example with certain and random road disturbances.

1. Introduction

Ride vibrations associated with a prolonged seating are the main risk factors for lumbago or backache, which seriously affect the mental and physical health of drivers or passengers and reduce their working efficiency. Thus, improving ride comfort which has developed as an applied science, is urgent. The first requirement to increase ride comfort is to attenuate the vibration transmission from the chassis to the driver. To achieve this goal, the vehicle seat suspension system plays an important role.

Between the human body and the automotive cabin, seat suspensions are not only to support the human body but also to isolate vibrations caused by rough road. Therefore, good seat suspension systems can significantly enhance ride comfort, which makes the seat suspension control become a hot topic. Recently, combining active vibration control mechanism with advanced control algorithms to design and analyze suspension systems has been a popular and effective way, and attracted considerable attention [1,2,6,8,14,18,25]. The core idea is to use active control method in suspension systems to reduce the impact of disturbance. This leads to the so-called active seat suspension system.

Most of the early studies for active seat suspension systems mainly confined their scope to vibration control of a rigid dummy mass on the seat. Without biodynamics included, it is clearly not precise enough to regard the complicated human body as a rigid mass for the individual difference. Various biomechanical models have been developed to describe the human motion, from 1 degree-of-freedom (DOF) to 15 DOF. These models can be grouped as lumped parameter models which consider the human body as several rigid bodies, springs and dampers.

Development of an active seat suspension system should be accompanied by the methodologies to control it, so that the design specifications can be satisfied. In general, the design specifications include two aspects for the active seat suspension system. The first one is ride comfort, which refers to isolating passengers from vibration and shock caused by road roughness. The second one can be seen as a constraint, limited suspension stroke, which means to keep suspension displacement within an allowable range. These two requirements are conflicting, for example, enhancing ride comfort results in larger suspension stroke, while an excessive suspension bottoming can lead to a considerable deterioration of ride comfort. Hence, extensive literature focuses on the choice of control methodologies to manage the trade-off between the two performance requirements, based on various control strategies, such as linear quadratic Gauss (LQG) [22,26], H_∞ control, [9,10] and adaptive control [4,13,19]. Among the proposed methods, the H_∞ active

* Corresponding author.
E-mail addresses: 1984sunweichao@gmail.com (W. Sun), lifking2009@gmail.com (J. Li), zhaoye8810@gmail.com (Y. Zhao), hjgao@hit.edu.cn (H. Gao).

0957-4158/$ - see front matter © 2010 Elsevier Ltd. All rights reserved.
doi:10.1016/j.mechatronics.2010.11.001

suspensions are intensively discussed in the context of robustness and disturbance attenuation.

In the existing literature, various control programs have been used in active seat suspension systems to isolate the force transmitted to the passengers. It is worth mentioning that most researchers design controllers for suspension systems over the entire frequency range, and the existing results ignore the fact that the vibrations, imported into the active seat suspension system, are mainly concentrated in the low frequency band. Meanwhile, the human body is more sensitive to vibrations of 4–8 Hz in the vertical direction, and human's organs will resonate with the vibrations in this frequency domain (ISO2361). Hence, the development of the finite frequency control is significative for active seat suspension systems. Accordingly, an interesting question would be whether we can design an H_∞ controller for active seat suspension systems in finite frequency domain, which can improve ride comfort as much as possible in the frequency sensitive domain 4–8 Hz. Although this seems to be a meaningful work, to the best of the authors' knowledge, few attempts have been made towards this direction, which motivates our present study.

Currently, the weighting function method which has been proved to be useful in practice, is the main strategy to deal with finite frequency problems. But it is weighting functions that increase the system complexity, and the process of selecting appropriate weights can be time-consuming as well. In the literature [16], the active seat suspension control is considered over the finite frequency domain, and the ride comfort is maximized by discriminatory minimization of average whole-body absorbed power over a hand of frequencies that causes most discomfort to a human being. The method used to deal with the problem of finite frequency is to add some weighting functions to the active seat suspension systems, which has been proved effective. However, this method is based on the appropriate weighting function as a precondition, and the choice of weighting function is quite time-consuming as mentioned before, especially when the designer has to shoot for a good trade-off between the complexity of the weights and the accuracy in capturing desired specifications.

Recently, a significant development made by Iwasaki and Hara is the generalized Kalman–Yakubovich–Popov (KYP) lemma [23] that establishes the equivalence between a frequency domain property and an linear matrix inequality (LMI) over a finite frequency range, allowing designers to impose performance requirements over chosen finite frequency ranges. The generalized KYP lemma is useful for the analysis and synthesis of practical application problems [3,11,15,24].

In addition, when all the states are on-line measurable, state feedback is an acceptable choice, as it can make use of full information, and thus the closed-loop performance can be enhanced to its full potential. However, state feedback control depends on the premise that all the state variables are on-line measurable, which leads into higher cost and additional complexity. In terms that not all the state variables can be measured on-line, output feedback control effects according to part of the measured states [12]. In other words, output feedback strategy requires less sensors, compared with the state feedback counterparts.

In this paper, the dynamic output feedback control of the active seat suspension system is investigated over the finite frequency range, where the human body is considered as a three DOF parameter models with rigid bodies, springs and dampers to increase the precision. By using the generalized KYP lemma, the finite frequency problems are transformed into a set of LMIs to be solved. In addition, the suspension deflection is limited within its allowed range to match the mechanical structure of the seat suspension. Finally, a practical example is employed to illustrate the effectiveness of the proposed method.

The remainder of this paper is organized as follows. The problem of finite frequency H_∞ controller design for active seat suspension systems based on the human body constitution is formulated in Section 2. Section 3 presents the design results of dynamic output feedback controllers. The simulation illustrating the usefulness and advantage of the proposed methodology is given in Section 4 and conclusions are given in Section 5.

Notation. For a matrix P, P^T, P^*, P^{-1} and $P^\perp$ denote its transpose, conjugate transpose, inverse and orthogonal complement, respectively; the notation $P > 0$ ($\geqslant 0$) means that P is real symmetric and positive definite (semi-definite); and $[P]_s$ means $P + P^T$. $\|G\|_\infty$ denotes the H_∞-norm of transfer function matrix $G(s)$. For matrices P and Q, $P \otimes Q$ means the Kronecker product. In symmetric block matrices or complex matrix expressions, we use an asterisk ($*$) to represent a term that is induced by symmetry and $diag\{\ldots\}$ stands for a block-diagonal matrix. Matrices, if their dimensions are not explicitly stated, are assumed to be compatible for algebraic operations.

2. Active seat suspension model

The problem of active seat suspension control is depicted in Fig. 1. It is known that an average human who subjects to vibration typically feels more discomfort over a certain band of frequencies. Since the seat suspension dynamics with human body on the seat can contribute much to the research of the improvement on ride comfort and safety, a mathematical human body model is strongly demanded for controller synthesis to alleviate the unwanted vibration and to mitigate the transmitted vibration energy.

The seated human body exposed to vibration is a sophisticated dynamic system whose mechanical properties are complex. This paper selects a three DOF model (see Fig. 2) that captures the essential dynamics of a seated human exposed to whole body vibration out of the great amount of seated human models based on the analytical study and experimental validation. It is found to be appropriate for the study of biodynamic responses of seated human subjects under vertical whole body vibration and also has a good trade-off between the complexity and the accuracy in capturing desired specifications [7,27].

The seat-driver model constituted by the seat suspension and human body shown in Fig. 1 is employed here for the purpose of analysis, whose detailed physical and biological structure is abstracted in Fig. 2. This linear model of seated human body was established by Wei and Griffin in 1998 [17], based on experimental results on live human bodies, which is constructed with two

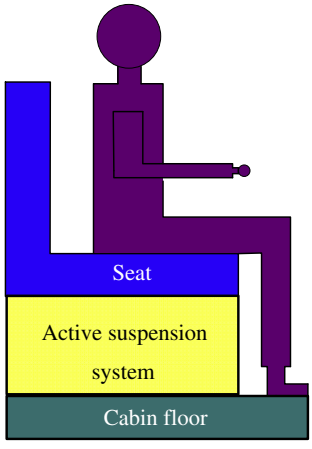

Fig. 1. The seat-driver model of 3 DOF.

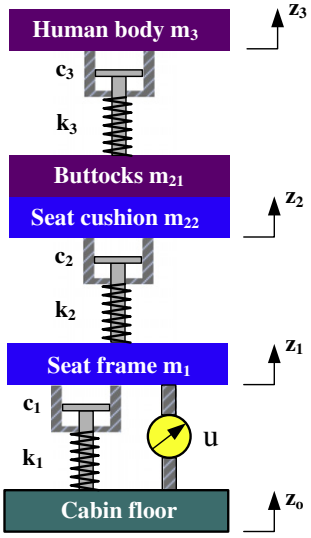

Fig. 2. The abstracted structure of active seat suspension system.

separate mass segments interconnected by a spring and a damper with a total mass of 51.2 kg. The mass of lower legs and feet is not included in this representation, due to their negligible contributions to the biodynamic response of the seated body. To predict the biodynamic responses more reasonably, the mass of buttocks and legs is assumed to contact rigidly with the seat. The road excitation input is transmitted to the cabin floor. It is assumed that only the vertical motion of the vehicle exists for simplification. Both pitching and rolling motions are neglected in this paper.

In Fig. 2, m_1 is the mass of seat frame; m_{21} and m_{22} are the masses of human thighs together with buttocks and the seat cushion, respectively, and $m_2 = m_{21} + m_{22}$; m_3 is the mass of the upper body of a seated human. c_1, c_2 and k_1, k_2 are dampings and stiffnesses of the passive suspension system, respectively; c_3 and k_3 stand for the damping and stiffness of the components inside human body such as spines; z_1, z_2 and z_3 are the displacements of the corresponding masses, respectively; z_0 is the road displacement input; u is the active control input of the seat suspension system.

The dynamic equations of motion of the seat suspension are given by:

$$\begin{aligned} m_1\ddot{z}_1 &= -c_1(\dot{z}_1-\dot{z}_0)-k_1(z_1-z_0)+c_2(\dot{z}_2-\dot{z}_1)+k_2(z_2-z_1)-u,\\ m_2\ddot{z}_2 &= -c_2(\dot{z}_2-\dot{z}_1)-k_2(z_2-z_1)+c_3(\dot{z}_3-\dot{z}_2)+k_3(z_3-z_2),\\ m_3\ddot{z}_3 &= -c_3(\dot{z}_3-\dot{z}_2)-k_3(z_3-z_2). \end{aligned} \tag{1}$$

Define the set of states and the disturbance input as follows:

$$\zeta(t) = \begin{bmatrix}\zeta_1^{\mathrm{T}}(t) & \zeta_2^{\mathrm{T}}(t) & \zeta_3^{\mathrm{T}}(t) & \zeta_4^{\mathrm{T}}(t) & \zeta_5^{\mathrm{T}}(t) & \zeta_6^{\mathrm{T}}(t)\end{bmatrix}^{\mathrm{T}},$$
$$w(t) = \dot{z}_0(t),$$

where the components of state variables are given as follows:

$$\begin{aligned} &\zeta_1(t) = z_1(t)-z_0(t), \quad \zeta_2(t) = \dot{z}_1(t),\\ &\zeta_3(t) = z_2(t)-z_1(t), \quad \zeta_4(t) = \dot{z}_2(t),\\ &\zeta_5(t) = z_3(t)-z_2(t), \quad \zeta_6(t) = \dot{z}_3(t). \end{aligned}$$

The dynamic equations in (1) can be rewritten in the following form:

$$\dot{\zeta}(t) = A\zeta(t) + Bu(t) + B_1 w(t),$$

where

$$A = \begin{bmatrix} 0 & 1 & 0 & 0 & 0 & 0\\ -\frac{k_1}{m_1} & -\frac{c_1+c_1}{m1} & \frac{k_2}{m_1} & \frac{c_2}{m_1} & 0 & 0\\ 0 & -1 & 0 & 1 & 0 & 0\\ 0 & \frac{c_2}{m_2} & -\frac{k_2}{m_2} & -\frac{c_2+c_3}{m_s} & \frac{k_3}{m_2} & \frac{c_3}{m_2}\\ 0 & 0 & 0 & -1 & 0 & 1\\ 0 & 0 & 0 & \frac{c_3}{m_3} & -\frac{k_3}{m_3} & -\frac{c_3}{m_3} \end{bmatrix},$$

$$B = \begin{bmatrix} 0\\ -\frac{1}{m_1}\\ 0\\ 0\\ 0\\ 0 \end{bmatrix}, \quad B_1 = \begin{bmatrix} -1\\ \frac{c_1}{m_1}\\ 0\\ 0\\ 0\\ 0 \end{bmatrix}.$$

Ride comfort can be characterized by body acceleration. As the main performance index, we formulate an H_∞ control problem to suppress disturbance. Denote body acceleration as control output $z_{o1}(t)$:

$$z_{o1}(t) = \ddot{z}_3(t).$$

Because of mechanical structure, suspension stroke should not exceed the allowable maximum $z_{\max}$, that is $|z_1 - z_0| < z_{\max}$. In order to satisfy the performance constraint, denote

$$z_{o2}(t) = \frac{z_1 - z_0}{z_{\max}},$$

as an output to be constrained.

Therefore, the vehicle suspension control system can be described as:

$$\begin{aligned} &\dot{\zeta}(t) = A\zeta(t) + Bu(t) + B_1 w(t),\\ &z_{o1}(t) = C_1\zeta(t) + D_1 u(t),\\ &z_{o2}(t) = C_2\zeta(t),\\ &y(t) = C\zeta(t), \end{aligned} \tag{2}$$

where

$$C_1 = \begin{bmatrix} 0 & 0 & 0 & \frac{c_3}{m_3} & -\frac{k_3}{m_3} & -\frac{c_3}{m_3} \end{bmatrix}, \quad D_1 = 0,$$

$$C_2 = \begin{bmatrix} \frac{1}{z_{\max}} & 0 & 0 & 0 & 0 & 0 \end{bmatrix},$$

$$C = \begin{bmatrix} 1 & 0 & 0 & 0 & 0 & 0\\ 0 & 0 & 1 & 0 & 0 & 0\\ 0 & 0 & 0 & 0 & 1 & 0 \end{bmatrix}.$$

Three sensors are installed to obtain the displacements ($\zeta_1(t)$, $\zeta_3(t)$ and $\zeta_5(t)$), and $y(t)$ is the measurable outputs.

Roughly speaking, traditional methods for the active seat suspension system considers the vibration suppression in the whole frequency band, which ignores the frequency requirements of the human body. Actually, the human body has different responses to different frequency vibrations, where vibrations over frequency 4–8 Hz are the major sources of the discomfort. In addition, though state feedback control is a powerful strategy, it is based on the premise that all the state variables are on-line measurable, which sometimes introduces higher cost and additional complexity by measuring all the states. In the cases where not all the state variables can be measured on-line, output feedback control is an alternative, which can conduct effective control according to part of the measured states. In other words, output feedback strategy requires less sensors, compared with the state feedback counterparts, and has been investigated in many studies.

In this paper, we design a dynamic output feedback H_∞ controller with the form:

$$\begin{aligned}\dot{\eta}(t) &= A_K\eta(t) + B_K y(t),\\ u(t) &= C_K\eta(t) + D_K y(t).\end{aligned} \tag{3}$$

According to the performance requirements, our goal can be summed up as follows:

$$\sup_{\varpi_1<\omega<\varpi_2} \|G(j\omega)\|_\infty < \gamma, \tag{4}$$

$$|z_{o2}(t)| \leqslant 1, \tag{5}$$

where $G(j\omega)$ represents the transfer function of the closed-loop systems from the disturbance input $w(t)$ to the controlled output $z_{o1}(t)$, and ϖ_1, ϖ_2 represent the upper and lower bounds of the chosen frequency.

3. Dynamic output feedback controller design

This section is devoted to the problem of finite frequency H_∞ controller design for the active seat suspension system in (2). We are interested in designing a dynamic output feedback controller, such that the H_∞ norm of the closed-loop system is minimized over the chosen frequency range, while respecting the constraint in (5) within bound.

Substituting (3) into (2), and defining $x(t) = [\zeta^{\mathrm{T}}(t) \quad \eta^{\mathrm{T}}(t)]^{\mathrm{T}}$, the closed-loop system admits the realization:

$$\begin{aligned}\dot{x}(t) &= \overline{A}x(t) + \overline{B}w(t),\\ z_{o1}(t) &= \overline{C}_1 x(t),\\ z_{o2}(t) &= \overline{C}_2 x(t),\end{aligned} \tag{6}$$

where

$$\overline{A} := \begin{bmatrix} A + BD_KC & BC_K \\ B_KC & A_K \end{bmatrix},\ \overline{B} := \begin{bmatrix} B_1 \\ 0 \end{bmatrix},\quad \overline{C}_1 := [C_1 + D_1D_KC \quad D_1C_K],\ \overline{C}_2 := [C_2 \quad 0]. \tag{7}$$

The transfer function of the closed-loop system from the disturbance input $w(t)$ to the controlled output $z_{o1}(t)$ is defined as follows:

$$G(j\omega) = \overline{C}_1(j\omega I - \overline{A})^{-1}\overline{B}.$$

3.1. Finite frequency case

In this subsection, a dynamic output feedback controller is designed in the finite frequency band, so that the closed-loop system in (6) is asymptotically stable, and satisfies

$$\sup_{\varpi_1<\omega<\varpi_2} \|G(j\omega)\|_\infty < \gamma, \tag{8}$$

while respecting the constraint in (5) within bound.

Theorem 1. *Give positive scalars γ, η, ρ and let a dynamic output feedback controller in the form of (3) be given. The closed-loop system in (6) is asymptotically stable, and satisfies $\sup_{\varpi_1<\omega<\varpi_2}\|G(j\omega)\|_\infty < \gamma$, while respecting the constraint in (5) with the disturbance energy under the bound $w_{max} = (\rho - V(0))/\eta$, if there exist symmetric matrices P, $P_s > 0$, $Q > 0$ and general matrix W satisfying*

$$\begin{bmatrix} [W]_s & -W^{\mathrm{T}}\overline{A} + P_s & -W^{\mathrm{T}} & -W^{\mathrm{T}}\overline{B} \\ * & -P_s & 0 & 0 \\ * & * & -P_s & 0 \\ * & * & * & -\eta I \end{bmatrix} < 0, \tag{9}$$

$$\begin{bmatrix} -\varpi_1\varpi_2 Q - \left[\overline{A}^{\mathrm{T}}W\right]_s & P - j\varpi_c Q + W^{\mathrm{T}} & -W^{\mathrm{T}}\overline{B} & \overline{C}_1^{\mathrm{T}} \\ P + j\varpi_c Q + W & -Q & 0 & 0 \\ -\overline{B}^{\mathrm{T}}W & 0 & -\gamma^2 I & 0 \\ \overline{C}_1 & 0 & 0 & -I \end{bmatrix} < 0, \tag{10}$$

$$\begin{bmatrix} -I & \sqrt{\rho}\overline{C}_2 \\ * & -P_s \end{bmatrix} < 0, \tag{11}$$

where $\varpi_c = (\varpi_1 + \varpi_2)/2$ is a given scalar.

Proof. By using Schur complement, inequality (9) is equivalent to

$$\begin{bmatrix} \frac{1}{\eta}W^{\mathrm{T}}\overline{B}\overline{B}^{\mathrm{T}}W + W^{\mathrm{T}}P_s^{-1}W + [W]_s & -W^{\mathrm{T}}\overline{A} + P_s \\ * & -P_s \end{bmatrix} < 0. \tag{12}$$

Performing the congruence transformation to inequality (12) by $diag\{-W^{-1}, P_s^{-1}\}$, with $W := -X^{-1}$, inequality (12) can be transformed to the following inequality:

$$\begin{bmatrix} \frac{1}{\eta}\overline{B}\overline{B}^{\mathrm{T}} + P_s^{-1} - [X]_s & \overline{A}P_s^{-1} + X^{\mathrm{T}} \\ * & -P_s^{-1} \end{bmatrix} < 0. \tag{13}$$

By using Lemma 2, inequality (13) is equivalent to

$$\overline{A}P_s^{-1} + P_s^{-1}\overline{A}^{\mathrm{T}} + \frac{1}{\eta}\overline{B}\overline{B}^{\mathrm{T}} < 0,$$

with $\Psi = \frac{1}{\eta}\overline{B}\overline{B}^{\mathrm{T}}$ and $S^{\mathrm{T}} = AP_s^{-1}$. Clearly, we have

$$\overline{A}^{\mathrm{T}}P_s + P_s\overline{A} + \frac{1}{\eta}P_s\overline{B}\overline{B}^{\mathrm{T}}P_s < 0, \tag{14}$$

which can guarantee $\overline{A}^{\mathrm{T}}P_s + P_s\overline{A} < 0$. From the standard Lyapunov theory for continuous-time linear system, the closed-loop system (6) is asymptotically stable with $w(t) = 0$. Note that (10) is equivalent to

$$[I \quad F_B]\Omega[I \quad F_B]^{\mathrm{T}} + [F_A W R]_s < 0, \tag{15}$$

where

$$F_A = \begin{bmatrix} -\overline{A}^{\mathrm{T}} \\ I \\ -\overline{B}^{\mathrm{T}} \end{bmatrix},\ F_B = \begin{bmatrix} \overline{C}_1^{\mathrm{T}} \\ 0 \\ 0 \end{bmatrix},\ R = \begin{bmatrix} I \\ 0 \\ 0 \end{bmatrix}^{\mathrm{T}},\ \Omega = T\begin{bmatrix} \Phi\otimes P + \Psi\otimes Q & 0 \\ 0 & \Pi \end{bmatrix}T^{\mathrm{T}},$$

$$\Pi = \begin{bmatrix} I & 0 \\ 0 & -\gamma^2 I \end{bmatrix},\ \Phi = \begin{bmatrix} 0 & 1 \\ 1 & 0 \end{bmatrix},\ \Psi = \begin{bmatrix} -1 & j\varpi_c \\ -j\varpi_c & -\varpi_1\varpi_2 \end{bmatrix},$$

with the permutation matrix T such as $[M_1 \quad M_2 \quad M_3 \quad M_4]\ T = [M_2 \quad M_1 \quad M_4 \quad M_3]$. From Lemma 1, (15) is equivalent to

$$F_A^{\perp}[I \quad F_B]\Omega[I \quad F_B]^{\mathrm{T}}F_A^{\perp^{\mathrm{T}}} < 0, \tag{16}$$

$$R^{\mathrm{T}^{\perp}}[I \quad F_B]\Omega[I \quad F_B]^{\mathrm{T}}R^{\mathrm{T}^{\perp^{\mathrm{T}}}} < 0, \tag{17}$$

where inequality (16) holds if and only if

$$F^{\mathrm{T}}\Omega F < 0, \tag{18}$$

with

$$F = \begin{bmatrix} I & \overline{A}^{\mathrm{T}} & 0 & \overline{C}_1^{\mathrm{T}} \\ 0 & \overline{B}^{\mathrm{T}} & I & 0 \end{bmatrix}^{\mathrm{T}}.$$

The inequality in (18) is equivalent to

$$\begin{bmatrix} \overline{A} & \overline{B} \\ I & 0 \\ \overline{C}_1 & 0 \\ 0 & I \end{bmatrix}^{\mathrm{T}} \begin{bmatrix} \Phi \otimes P + \Psi \otimes Q & 0 \\ 0 & \Pi \end{bmatrix} \begin{bmatrix} \overline{A} & \overline{B} \\ I & 0 \\ \overline{C}_1 & 0 \\ 0 & I \end{bmatrix} < 0, \tag{19}$$

which is further equivalent to

$$\begin{bmatrix} \overline{A} & \overline{B} \\ I & 0 \end{bmatrix}^{\mathrm{T}} (\Phi \otimes P + \Psi \otimes Q) \begin{bmatrix} \overline{A} & \overline{B} \\ I & 0 \end{bmatrix} + \begin{bmatrix} \overline{C}_1 & 0 \\ 0 & I \end{bmatrix}^{\mathrm{T}} \Pi \begin{bmatrix} \overline{C}_1 & 0 \\ 0 & I \end{bmatrix} < 0. \tag{20}$$

By using Lemma 3, the above inequality is equivalent to

$$\begin{bmatrix} (j\omega I - \overline{A})^{-1}\overline{B} \\ I \end{bmatrix}^{*} \begin{bmatrix} \overline{C}_1 & 0 \\ 0 & I \end{bmatrix}^{*} \Pi \begin{bmatrix} \overline{C}_1 & 0 \\ 0 & I \end{bmatrix} \begin{bmatrix} (j\omega I - \overline{A})^{-1}\overline{B} \\ I \end{bmatrix} < 0, \ \varpi_1 < \omega < \varpi_2, \tag{21}$$

which is equivalent to the finite frequency H_∞ performance index inequality

$$\sup_{\varpi_1 < \omega < \varpi_2} \|G(j\omega)\|_\infty < \gamma. \tag{22}$$

Denote $V(t) = x^{\mathrm{T}}(t)P_s x(t)$ as the energy function, whose derivative is obtained as

$$\dot{V}(t) = 2x^{\mathrm{T}}(t)P_s\overline{A}x(t) + 2x^{\mathrm{T}}(t)P_s\overline{B}w(t).$$

Noting that

$$2x^{\mathrm{T}}(t)P_s\overline{B}w(t) \leqslant \frac{1}{\eta}x^{\mathrm{T}}(t)P_s\overline{B}\overline{B}^{\mathrm{T}}P_s x(t) + \eta w^{\mathrm{T}}(t)w(t), \forall \eta > 0,$$

we have

$$\dot{V}(t) \leqslant x^{\mathrm{T}}(t)(\overline{A}^{\mathrm{T}}P_s + P_s\overline{A} + \frac{1}{\eta}P_s\overline{B}\overline{B}^{\mathrm{T}}P_s)x(t) + \eta w^{\mathrm{T}}(t)w(t).$$

According to inequality (14), we have

$$\dot{V}(t) \leqslant \eta w^{\mathrm{T}}(t)w(t).$$

Integrating both sides of the above inequality from 0 to t results in

$$V(t) - V(0) \leqslant \eta \int_0^t w^{\mathrm{T}}(t)w(t)dt \leqslant \eta\|w\|_2^2 = \eta w_{\max}.$$

This shows that

$$x^{\mathrm{T}}(t)P_s x(t) \leqslant V(0) + \eta w_{\max} = \rho. \tag{23}$$

Consider

$$\max_{t\geqslant 0}|z_{o2}(t)|^2 = \max_{t\geqslant 0}\|x^{\mathrm{T}}(t)\overline{C}_2^{\mathrm{T}}\overline{C}_2 x(t)\|_2.$$

Using the transformation $\bar{x}(t) = \overline{P}_s^{\frac{1}{2}}x(t)$, from inequality (23) it follows that

$$\bar{x}^{\mathrm{T}}(t)\bar{x}(t) \leqslant \rho.$$

Hence,

$$\max_{t\geqslant 0}|z_{o2}(t)|^2 = \max_{t\geqslant 0}\left\|\bar{x}^{\mathrm{T}}(t)P_s^{-\frac{1}{2}}\overline{C}_2^{\mathrm{T}}\overline{C}_2 P_s^{-\frac{1}{2}}\bar{x}^{\mathrm{T}}(t)\right\|_2 \leqslant \rho\cdot\lambda_{\max}(P_s^{-\frac{1}{2}}\overline{C}_2^{\mathrm{T}}\overline{C}_2 P_s^{-\frac{1}{2}}), \tag{24}$$

where $\lambda_{\max}(\cdot)$ represents the maximum eigenvalue. Then, the constraint in (5) holds if

$$\rho P_s^{-\frac{1}{2}}\overline{C}_2^{\mathrm{T}}\overline{C}_2 P_s^{-\frac{1}{2}} < I, \tag{25}$$

which, by Schur complement, is equivalent to (11). The proof is completed. □

Expressions in Theorem 1 are non-convex due to the product terms of the multiplier W, the controller parameters and coefficient matrices. In order to solve this problem, we carry on the following transformation.

In accordance with the partition of $\overline{A}$ in (7), we introduce a partition of W and its inverse W^{-1} in the form:

$$W = \begin{bmatrix} X & Y \\ U & V \end{bmatrix}, \ W^{-1} = \begin{bmatrix} M & G \\ H & L \end{bmatrix}. \tag{26}$$

From the literature [21], there is no loss of generality in assuming that U and H are invertible. Define

$$\Delta_1 = \begin{bmatrix} X & I \\ U & 0 \end{bmatrix}, \ \Delta_2 = \begin{bmatrix} I & M \\ 0 & H \end{bmatrix},$$

and note that

$$W\Delta_2 = \Delta_1. \tag{27}$$

Define

$$J_1 = diag\{\Delta_2^{\mathrm{T}}, \Delta_2^{\mathrm{T}}, \Delta_2^{\mathrm{T}}, I\}, \ J_2 = diag\{\Delta_2^{\mathrm{T}}, \Delta_2^{\mathrm{T}}, I, I\}, \ J_3 = diag\{I, \Delta_2^{\mathrm{T}}\}.$$

Pre- and post-multiplying (9)–(11) by J_1, J_2 and J_3 and their transposes, respectively, and defining

$$\overline{Q} = \Delta_2^{\mathrm{T}}Q\Delta_2, \ \overline{P} = \Delta_2^{\mathrm{T}}P\Delta_2, \ \overline{P}_s = \Delta_2^{\mathrm{T}}P_s\Delta_2,$$

$$\widehat{A} = \Delta_2^{\mathrm{T}}W^{\mathrm{T}}\overline{A}\Delta_2 = \begin{bmatrix} X^{\mathrm{T}}A + \widehat{B}_K C & \widehat{A}_K \\ A + B\widehat{D}_K C & AM + B\widehat{C}_K \end{bmatrix},$$

$$\widehat{B} = \Delta_2^{\mathrm{T}}W^{\mathrm{T}}\overline{B} = \begin{bmatrix} X^{\mathrm{T}}B_1 \\ B_1 \end{bmatrix},$$

$$\widehat{C}_1 = \overline{C}_1\Delta_2 = \begin{bmatrix} C_1 + D_1\widehat{D}_K C & C_1 M + D_1\widehat{C}_K \end{bmatrix},$$

$$\widehat{C}_2 = \overline{C}_2\Delta_2 = [C_2 \quad C_2 M],$$

$$\overline{W} = \Delta_2^{\mathrm{T}}W\Delta_2 = \begin{bmatrix} X^{\mathrm{T}} & Z \\ I & M \end{bmatrix},$$

with the following linearizing changes of variables:

$$\widehat{A}_K = X^{\mathrm{T}}AM + X^{\mathrm{T}}BD_K CM + U^{\mathrm{T}}B_K CM + X^{\mathrm{T}}BC_K H + U^{\mathrm{T}}A_K H, \tag{28}$$

$$\widehat{B}_K = X^{\mathrm{T}}BD_K + U^{\mathrm{T}}B_K, \tag{29}$$

$$\widehat{C}_K = C_K H + D_K CM, \tag{30}$$

$$\widehat{D}_K = D_K, \tag{31}$$

$$Z = X^{\mathrm{T}}M + U^{\mathrm{T}}H, \tag{32}$$

we can give the following theorem.

Theorem 2. *Give positive scalars γ,η,ρ. A dynamic output feedback controller in the form of (3) exists, such that the closed-loop system in (6) is asymptotically stable, and satisfies $\sup_{\varpi_1<\omega<\varpi_2}\|G(j\omega)\|_\infty < \gamma$, while respecting the constraint in (5) with the disturbance energy under the bound $w_{max} = (\rho - V(0))/\eta$, if there exist symmetric matrices $\overline{P}$, $\overline{P}_s > 0$, $\overline{Q} > 0$ and general matrices $\overline{W}$, $\widehat{A}_k$, $\widehat{B}_k$, $\widehat{C}_k$, $\widehat{D}_k$, M, X and Z satisfying*

$$\begin{bmatrix} [\overline{W}]_s & -\widehat{A} + \overline{P}_s & -\overline{W}^{\mathrm{T}} & -\widehat{B} \\ * & -\overline{P}_s & 0 & 0 \\ * & * & -\overline{P}_s & 0 \\ * & * & * & -\eta I \end{bmatrix} < 0, \tag{33}$$

$$\begin{bmatrix} -\varpi_1\varpi_2\overline{Q}-[\widehat{A}]_s & \overline{P}-j\varpi_c\overline{Q}+\overline{W}^{\mathrm{T}} & -\widehat{B} & \widehat{C}_1^{\mathrm{T}} \\ \overline{P}+j\varpi_c\overline{Q}+\overline{W} & -\overline{Q} & 0 & 0 \\ -\widehat{B}^{\mathrm{T}} & 0 & -\gamma^2 I & 0 \\ \widehat{C}_1 & 0 & 0 & -I \end{bmatrix} < 0, \tag{34}$$

$$\begin{bmatrix} -I & \sqrt{\rho}\widehat{C}_2 \\ * & -\overline{P}_s \end{bmatrix} < 0. \tag{35}$$

Moreover, if the above inequalities has a feasible solution, then the matrices $\widehat{A}_k$, $\widehat{B}_k$, $\widehat{C}_k$, $\widehat{D}_k$, M, X and Z can be obtained. According to (28)–(31), we will compute the controller by

$$\begin{aligned} D_K &= \widehat{D}_K, \\ C_K &= (\widehat{C}_K - D_K C M)H^{-1}, \\ B_K &= U^{-\mathrm{T}}(\widehat{B}_K - X^{\mathrm{T}} B D_K), \\ A_K &= U^{-\mathrm{T}}\left[\widehat{A}_K - X^{\mathrm{T}} A M - X^{\mathrm{T}} B D_K C M - U^{\mathrm{T}} B_K C M - X^{\mathrm{T}} B C_K H\right] H^{-1}. \end{aligned} \tag{36}$$

Remark 1. Note that the linear matrix inequality in (34) has complex variables. According to [20], the LMI in complex variables can be converted to an LMI of larger dimension in real variables. This means that inequality $S_1 + jS_2 < 0$ is equivalent to $\begin{bmatrix} S_1 & S_2 \\ -S_2 & S_1 \end{bmatrix} < 0$. Based on the above method, inequality (34) can be split into

$$\begin{bmatrix} -\varpi_1\varpi_2\overline{Q}-[\widehat{A}]_s & \overline{P}+\overline{W}^{\mathrm{T}} & -\widehat{B} & \widehat{C}_1^{\mathrm{T}} \\ * & -\overline{Q} & 0 & 0 \\ * & * & -\gamma^2 I & 0 \\ * & * & * & -I \end{bmatrix} + j\begin{bmatrix} 0 & -\varpi_c\overline{Q} & 0 & 0 \\ \varpi_c\overline{Q} & 0 & 0 & 0 \\ 0 & 0 & 0 & 0 \\ 0 & 0 & 0 & 0 \end{bmatrix} < 0, \tag{37}$$

which can be solved by

$$\begin{bmatrix} -\varpi_1\varpi_2\overline{Q}-[\widehat{A}]_s & \overline{P}+\overline{W}^{\mathrm{T}} & -\widehat{B} & \widehat{C}_1^{\mathrm{T}} & 0 & -\varpi_c\overline{Q} & 0 & 0 \\ * & -\overline{Q} & 0 & 0 & \varpi_c\overline{Q} & 0 & 0 & 0 \\ * & * & -\gamma^2 I & 0 & 0 & 0 & 0 & 0 \\ * & * & * & -I & 0 & 0 & 0 & 0 \\ * & * & * & * & -\varpi_1\varpi_2\overline{Q}-[\widehat{A}]_s & \overline{P}+\overline{W}^{\mathrm{T}} & -\widehat{B} & \widehat{C}_1^{\mathrm{T}} \\ * & * & * & * & * & -\overline{Q} & 0 & 0 \\ * & * & * & * & * & * & -\gamma^2 I & 0 \\ * & * & * & * & * & * & * & -I \end{bmatrix} < 0. \tag{38}$$

Remark 2. When we calculate the controller, the matrices U and H, which cannot be directly obtained by the Theorem 2, are needed and they should be chosen such that

$$U^{\mathrm{T}}H = Z - X^{\mathrm{T}}M.$$

It is worth mentioning that the factorization of $U^{\mathrm{T}}H$ can always be achieved so that the invertible matrices U and H are deduced. In this paper, the two invertible matrices are obtained by using the singular value decomposition approach.

3.2. Entire frequency case

In order to highlight the advantages of the finite frequency controller, we design another dynamic output feedback controller in the entire frequency domain, based on the method proposed in the literature [5]. In this subsection, a dynamic output feedback controller is designed over the entire frequency range, so that the closed-loop system in (6) is asymptotically stable, and satisfies

$$\sup_{-\infty<\omega<+\infty} \|G(j\omega)\|_\infty < \gamma, \tag{39}$$

while respecting the constraint in (5) within bound. The performance index (39) can be further expressed as: under zero initial condition, the closed-loop system guarantees that $\|z_{o1}\|_2 < \gamma\|w\|_2$ for all nonzero $w \in L_2[0,\infty)$.

Corollary 1. *Let positive scalars ρ, γ be given. If there exists symmetric matrix $P_c > 0$ satisfying*

$$\begin{bmatrix} [P_c\overline{A}]_s & P_c\overline{B} & \overline{C}_1^{\mathrm{T}} \\ * & -\gamma^2 I & 0 \\ * & * & -I \end{bmatrix} < 0, \tag{40}$$

$$\begin{bmatrix} -I & \sqrt{\rho}\overline{C}_2 \\ * & -P_c \end{bmatrix} < 0, \tag{41}$$

then a stabilizing dynamic output feedback controller in the form of (3) exists, such that

1. *the closed-loop system in (6) is asymptotically stable;*
2. *under zero initial condition, the closed-loop system guarantees that $\|z_{o1}\|_2 < \gamma\|w\|_2$ for all nonzero $w \in L_2[0,\infty)$;*
3. *the constraint in (5) is guaranteed with the disturbance energy under the bound $w_{max} = (\rho - V(0))/\gamma^2$.*

Proof. Since the results can easily be obtained, the proof has been omitted here. □

Hereafter, we will show how to transform (40) and (41) into the forms which can be solved directly. Partition the matrix P_c and its inverse P_c^{-1} in the form

$$P_c = \begin{bmatrix} Y_c & N_c \\ N_c^{\mathrm{T}} & \# \end{bmatrix}, \; P_c^{-1} = \begin{bmatrix} X_c & M_c \\ M_c^{\mathrm{T}} & \# \end{bmatrix}, \tag{42}$$

where "#" represents this position can be arbitrary. From the literature [5], there is no loss of generality in assuming that N_c and M_c are invertible. Define

$$\Delta_{c1} = \begin{bmatrix} X_c & I \\ M_c^{\mathrm{T}} & 0 \end{bmatrix}, \; \Delta_{c2} = \begin{bmatrix} I & Y_c \\ 0 & N_c^{\mathrm{T}} \end{bmatrix},$$

and note that

$$P_c\Delta_{c1} = \Delta_{c2}. \tag{43}$$

Define

$$J_{c1} = diag\{\Delta_{c1}, I, I\},\ J_{c2} = diag\{I, \Delta_{c1}\}.$$

Pre- and post-multiplying (40) and (41) by J_{c1} and J_{c2} and their transposes, respectively, and defining

$$\overline{A}_e = \Delta_{c1}^{\mathrm{T}} P_c \overline{A} \Delta_2 = \begin{bmatrix} AX_c + B\widehat{C}_c & A + B\widehat{D}_c C \\ \widehat{A}_c & Y_c A + \widehat{B}_c C \end{bmatrix},$$

$$\overline{B}_e = \Delta_{c1}^{\mathrm{T}} P_c \overline{B} = \begin{bmatrix} B_1 \\ Y_c B_1 \end{bmatrix},$$

$$\overline{C}_{e1} = \overline{C}_1 \Delta_{c1} = \begin{bmatrix} C_1 X_c + D_1 \widehat{C}_c & C_1 + D_1 \widehat{D}_c C \end{bmatrix},$$

$$\overline{C}_{e2} = \overline{C}_2 \Delta_{c1} = [C_2 X_c \quad C_2],$$

$$\overline{P}_c = \Delta_{c1}^{\mathrm{T}} P_c \Delta_{c1} = \begin{bmatrix} X_c & I \\ I & Y_c \end{bmatrix},$$

with the following linearizing changes of variables:

$$\begin{aligned} \widehat{A}_c &= Y_c A X_c + Y_c B \widehat{D}_c C X_c + N_c B_K C X_c + Y_c B C_K M_c^{\mathrm{T}} + N_c A_K M_c^{\mathrm{T}}, \\ \widehat{B}_c &= Y_c B \widehat{D}_c + N_c B_K, \\ \widehat{C}_c &= C_K M_c^{\mathrm{T}} + \widehat{D}_c C X_c, \\ \widehat{D}_c &= D_K, \end{aligned} \tag{44}$$

we can give the following corollary:

Corollary 2. *Let scalar $\gamma > 0$ be given. If there exist matrices $Y_c > 0, X_c > 0$ and general matrices $\widehat{A}_c$, $\widehat{B}_c$, $\widehat{C}_c$, $\widehat{D}_c$ satisfying*

$$\begin{bmatrix} [\overline{A}_e]_s & \overline{B}_e & \overline{C}_{e1}^{\mathrm{T}} \\ * & -\gamma^2 I & 0 \\ * & * & -I \end{bmatrix} < 0, \tag{45}$$

$$\begin{bmatrix} -I & \sqrt{\rho}\overline{C}_{e2} \\ * & -\overline{P}_c \end{bmatrix} < 0. \tag{46}$$

then a stabilizing dynamic output feedback controller in the form of (3) exists, such that

1) *the closed-loop system in (6) is asymptotically stable;*
2) *under zero initial condition, the closed-loop system guarantees that $\|z_{o1}\|_2 < \gamma \|w\|_2$ for all nonzero $w \in L_2[0,\infty)$;*
3) *the constraint in (5) is guaranteed with the disturbance energy under the bound $w_{max} = (\rho - V(0))/\gamma^2$.*

Moreover, if inequalities (45) and (46) have a feasible solution, then we will compute the controller by

$$\begin{aligned} D_K &= \widehat{D}_c, \\ C_K &= (\widehat{C}_c - \widehat{D}_c C X_c) M_c^{-\mathrm{T}}, \\ B_K &= N_c^{-1}(\widehat{B}_c - Y_c B \widehat{D}_c), \\ A_K &= N_c^{-1}[\widehat{A}_c - Y_c A X_c - Y_c B \widehat{D}_c C X_c - N_c B_K C X_c - Y_c B C_K M_c^{\mathrm{T}}] M_c^{-\mathrm{T}}. \end{aligned} \tag{47}$$

Remark 3. As the same lines with Remark 2, the matrices N_c and M_c, which cannot be directly obtained by the Corollary 2, should satisfy

$$N_c M_c^{\mathrm{T}} = I - Y_c X_c.$$

Here, we also obtain the two invertible matrices by using the singular value decomposition approach.

4. A design example

In this section, we will apply the above approach to design a dynamic output feedback H_∞ controller in the finite frequency domain based on the active seat suspension model described in Section 2. The parameters are listed in Table 1:

Firstly, the closed-loop system with a dynamic output feedback H_∞ controller in the finite frequency domain can be obtained, based on the proposed method in Section 2, and we denote this closed-loop system as system Σ_1 for brevity. After solving the matrix inequalities (33)–(35) for symmetric matrices $\overline{P}$, $\overline{P}_s > 0$, $\overline{Q} > 0$ and general matrices $\overline{W}$, $\widehat{A}_k$, $\widehat{B}_k$, $\widehat{C}_k$, $\widehat{D}_k$, M, X and Z with given scalars $\gamma > 0$ and $\varpi_1 = 8\pi$rad/s (4 Hz), $\varpi_2 = 16\pi$rad/s (8 Hz), $\eta = 10000$, the optimal guaranteed closed-loop H_∞ performance obtained is

$$\gamma_{\min} = 3.1718.$$

Then, the parameter matrices of the dynamic output feedback controller which are shown in Appendix B, are obtained.

For subsequent comparison, we can get another closed-loop system with a dynamic output feedback H_∞ controller over the entire frequency range, according to the Corollary 2, and set it as system Σ_2. After solving the matrix inequalities in Corollary 2, we obtain the optimal guaranteed closed-loop H_∞ performance:

$$\gamma_{\min} = 4.8113.$$

The parameter matrices of the dynamic output feedback controller in entire frequency domain are also listed in Appendix B.

In order to further illustrate the effectiveness of disturbance suppression over the frequency band 4–8 Hz, the curves of maximum singular values are drawn in Fig. 3, where the open-loop system (passive mode), the closed-loop system Σ_1 (active finite frequency mode) and the closed-loop system Σ_2 (active entire frequency mode), are compared. In Fig. 3, the dash-dot/dot/solid line

Table 1
Model parameters of the active seat suspension system

Mass (kg)		Damping coefficient (N s/m)		Spring constant (N/m)	
m_1	15	c_1	830	k_1	31,000
m_2	(1 + 7.8)	c_2	200	k_2	18,000
m_3	43.8	c_3	1485	k_3	44,130

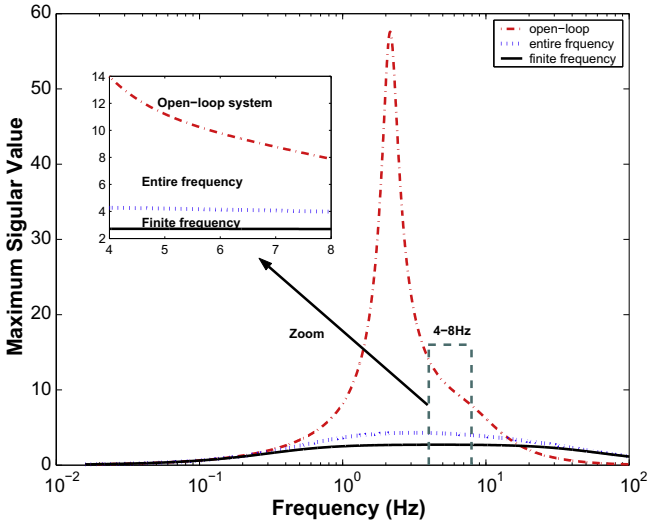

Fig. 3. The curves of maximum singular values (blue line: open-loop system; red line: system Σ_2; black line: system Σ_1). (For interpretation of the references to colour in this figure legend, the reader is referred to the web version of this article.)

represents the curve of maximum singular values in the open-loop system/system Σ_2/system Σ_1, respectively. From Fig. 3, we can see that the closed-loop system with finite frequency controller has the least value of H_∞ norm over the frequency range 4–8 Hz, compared with the passive system and the closed-loop system with an entire frequency controller, which means an improved ride comfort has been achieved by the finite frequency controller.

Evaluation of the vehicle seat suspension performance is based on the examination of two response quantities, that is, the body acceleration of the specific frequency domain and the suspension deflection between the cabin floor and seat frame. In order to evaluate the suspension characteristics with respect to the two performance requirements, both certain and random inputs are employed in this simulation.

4.1. Deterministic simulation

It is assumed that the certain disturbance input has the following form:

$$w(t) = \begin{cases} A\sin(2\pi ft), & \text{if } 0 \leqslant t \leqslant T, \\ 0, & \text{if } t > T, \end{cases} \tag{48}$$

where A, f and $T = 1/f$ represent the amplitude, frequency and period of vibration, respectively. Assume $A = 0.5$ m, and the simulations are given by setting the disturbance frequency as 4 Hz, 8 Hz, respectively. The time-domain responses of body vertical acceleration for the active seat suspension system are shown in Figs. 4 and 5, where the solid/dot lines are the responses of body vertical acceleration with the finite/entire frequency controller, and the dash-dot lines respect the responses of the passive system. It is seen from these two figures that the magnitudes for the body accelerations are significantly decreased. Also, the accelerations for the finite frequency controlled active seat suspension vanish faster than the other two suspensions (passive suspension and entire frequency controlled suspension). These results confirm the efficiency of the finite frequency controller. In particular, reduced accelerations indicate that the ride comfort is improved. In addition, Fig. 6 shows that the ratio $(z_1 - z_0)/z_{\max}$ is below 1, which means the time-domain constraint is guaranteed by the designed controller.

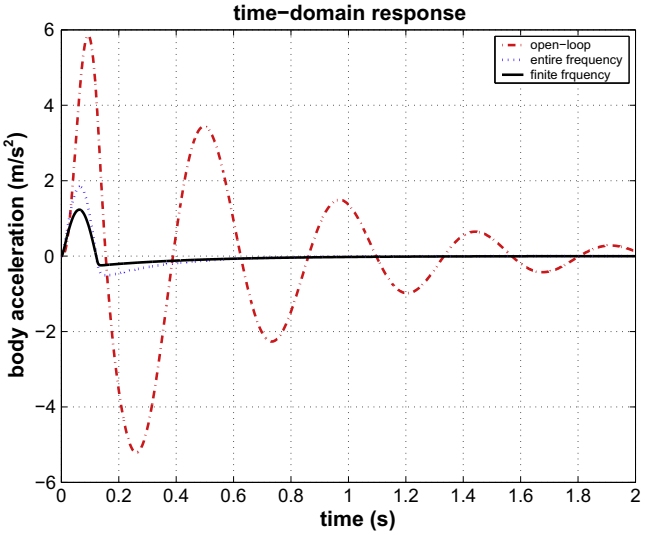

Fig. 4. The time-domain response of body acceleration ($f = 4$ Hz).

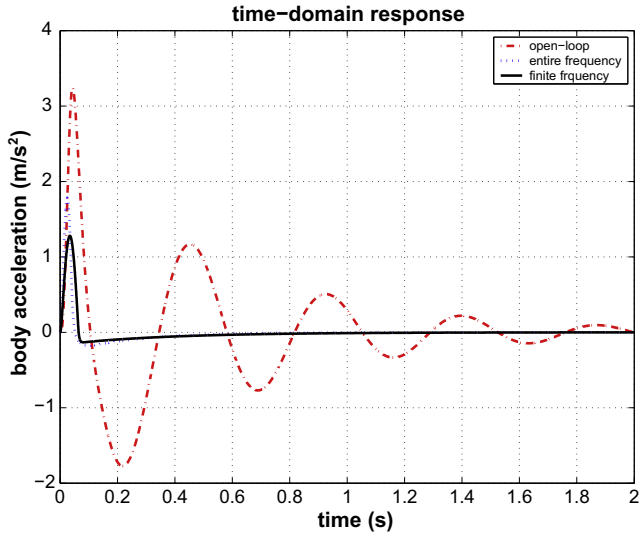

Fig. 5. The time-domain response of body acceleration ($f = 8$ Hz).

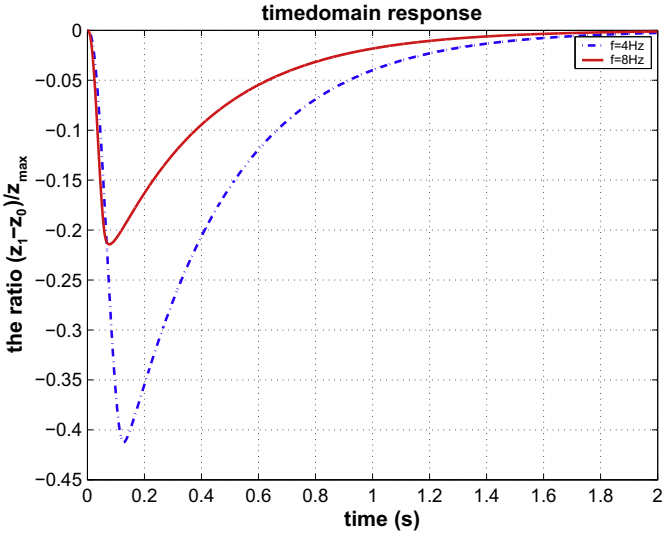

Fig. 6. The time-domain constraint (the ratio $(z_1 - z_0)/z_{\max}$).

4.2. Random signal simulation

Random vibrations are consistent and typically specified as random process with a given ground displacement power spectral density (PSD) of

$$G_q(n) = G_q(n_0)\left(\frac{n}{n_0}\right)^{-W}, \tag{49}$$

where n is the spatial frequency and n_0 is the reference spatial frequency of $n_0 = 0.1(1/\text{m})$; $G_q(n_0)$ stands for the road roughness coefficient; $W = 2$ is the road roughness constant. Related to the time frequency f, we have $f = nV$ with V for the vehicle forward velocity. According to (49), we can obtain the PSD ground displacement:

$$G_q(f) = G_q(n_0)n_0^2\frac{V}{f^2}. \tag{50}$$

Correspondingly, PSD ground velocity is given by

$$G_{\dot q}(f) = (2\pi f)^2 G_q(f) = 4\pi G_q(n_0)n_0^2 V, \tag{51}$$

which is only related with the vehicle forward velocity. When the vehicle forward velocity is fixed, the ground velocity can be viewed

as a white-noise signal. Select the road roughness as $G_q(n_0) = 256 \times 10^{-6}\ m^3$, which is corresponded to D Grade (Poor) according to ISO2361 standards, to generate the random road profile. Set the vehicle forward velocity as $V = 45$ km/h, and as expected, it is observed from Fig. 7 that the closed-loop system Σ_1 with finite frequency controller realizes a better ride comfort, compared with system Σ_2 over the frequency range 4–8 Hz (since the system Σ_1 has lower PSD body acceleration than system Σ_2, and smaller PSD body acceleration value results in better ride comfort), where PSD body acceleration can be calculated by

$$G_{z_1}(f) = |G(j\omega)|^2 G_{\dot{q}}(f). \tag{52}$$

To check more random road profiles, we select the road roughness as $G_q(n_0) = 16 \times 10^{-6}\ m^3$ (B Grade, Good), $G_q(n_0) = 64 \times 10^{-6}\ m^3$ (C Grade, Average), and $G_q(n_0) = 1024 \times 10^{-6}\ m^3$ (E Grade, Very Poor), respectively. From Fig. 8, it can be observed that system Σ_1 realizes a better ride comfort in spite of the different road roughness.

With the series of simulations above, a fact is proved once again: In the selected frequency domain, the finite frequency method is superior to the entire frequency method in the capability of disturbance suppression. The reason for this is that the finite frequency approach concentrates control powers on the chosen frequency domain and relaxes the restrictions of the other frequencies, by imposing the frequency band constraints in the performance indicators.

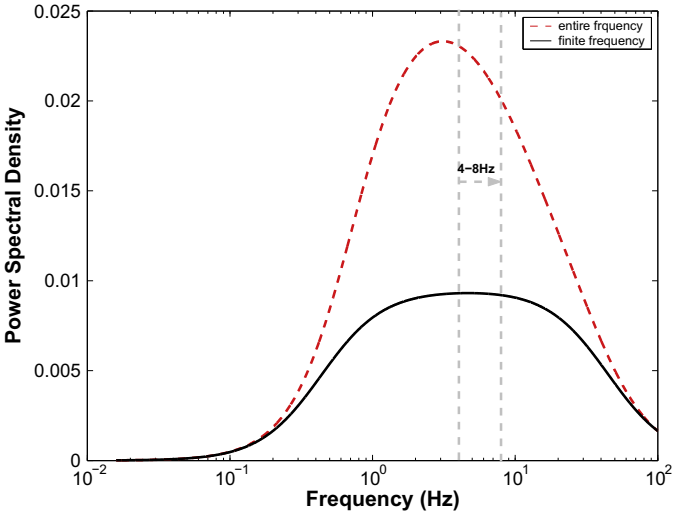

Fig. 7. The power spectral density of body acceleration (system Σ_1: black line; system Σ_2: red line). (For interpretation of the references to colour in this figure legend, the reader is referred to the web version of this article.)

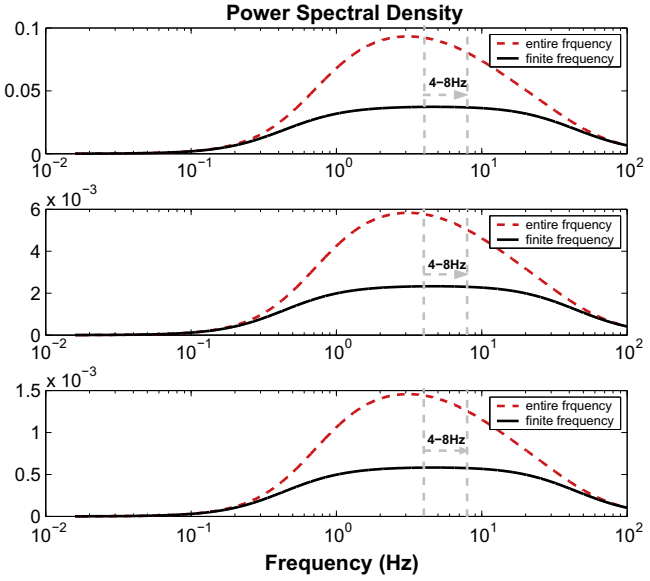

Fig. 8. The power spectral density of body acceleration for four kinds of road profiles.

5. Concluding remarks

In this paper, a dynamic output feedback H_∞ controller for active seat suspension system has been designed, which can suit people's physical structure to improve ride comfort as much as possible. The key idea of designing the proposed controller is to use the generalized Kalman–Yakubovich–Popov (GKYP) lemma and the linearizing change of variables. In addition, the limited suspension stroke is guaranteed by considering this constraint in the controller design. The simulation results show that the finite frequency controller achieves better disturbance attenuation for the concerned frequency range, and the performance constraint is also guaranteed.

Acknowledgements

This work was supported in part by the 973 Project (2009CB320600), the National Natural Science Foundation of China (60825303), the Heilongjiang Outstanding Youth Science Fund (JC200809). the Foundation for the Author of National Excellent Doctoral Dissertation of China (2007E4), the Fok Ying Tung Education Foundation (111064) and the Key Laboratory of Integrated Automation for the Process Industry (Northeastern University), Ministry of Education.

Appendix A

Lemma 1. *(Projection Lemma [21]): Let Γ,Λ,Θ be given there exists a matrix F satisfying*

$$\Gamma F \Lambda + (\Gamma F \Lambda)^{\mathrm{T}} + \Theta < 0,$$

if and only if the following two conditions hold

$$\Gamma^{\perp}\Theta\Gamma^{\perp^{\mathrm{T}}} < 0,\ \Lambda^{\mathrm{T}^{\perp}}\Theta\Lambda^{\mathrm{T}^{\perp^{\mathrm{T}}}} < 0.$$

Lemma 2. *(Reciprocal Projection Lemma [21]): Let P be any given positive definite matrix. The following statements are equivalent:*

(1) $\Psi + S + S^{\mathrm{T}} < 0$.

(2) *The LMI problem*

$$\begin{bmatrix} \Psi + P - [X]_s & S^{\mathrm{T}} + X^{\mathrm{T}} \\ * & -P \end{bmatrix} < 0$$

is feasible with respect to X.

Lemma 3. *(Generalized KYP Lemma [15]): Let matrices Θ,F and Φ,Ψ be given. Denote by N_ω the null space of $T_\omega F$, where $T_\omega = [I \quad -j\omega I]$. The inequality*

$$N_\omega^* \Theta N_\omega < 0,\ \text{with}\ \omega \in [\varpi_1\ \varpi_2],$$

holds if and only if there exist P, Q > 0, such that

$$F^*(\Phi \otimes P + \Psi \otimes Q)F < 0,$$

where

$$\Phi = \begin{bmatrix} 0 & 1 \\ 1 & 0 \end{bmatrix},\ \Psi = \begin{bmatrix} -1 & j\varpi_c \\ -j\varpi_c & -\varpi_1\varpi_2 \end{bmatrix},$$

with $\varpi_c = (\varpi_1 + \varpi_2)/2$.

Appendix B

The resulting parameter matrices of the dynamic output feedback controller in finite frequency domain:

$$A_{Kf}=\begin{bmatrix} -4296.4 & -393.53 & -39.999 & 9.1582 & -3.6152 & -0.48456 \\ -40632 & -3765.5 & -380.16 & 86.833 & -34.351 & -4.6028 \\ 1.9431\times10^{5} & 18942 & 1822.6 & -444.89 & 172.32 & 23.006 \\ 1.7516\times10^{5} & 5146.3 & 1120.1 & -331.81 & 101.65 & 14.557 \\ 9.0486\times10^{6} & 2.6433\times10^{5} & 48716 & -8547 & 3599.8 & 517.92 \\ 1.122\times10^{7} & 7.7148\times10^{7} & 2.2219\times10^{7} & -2.4638\times10^{6} & -2.7647\times10^{5} & -42379 \end{bmatrix},$$

$$B_{Kf}=\begin{bmatrix} 215.73 & -1.2399 & -24.844 \\ 2049.1 & -11.324 & -235.43 \\ -10195 & 124.01 & 1178.3 \\ -6563.4 & -677.16 & -4434.9 \\ -2.0397\times10^{5} & 79809 & -76930 \\ -9.9297\times10^{7} & 3.8266\times10^{6} & 6.5246\times10^{5} \end{bmatrix},$$

$$C_{Kf}=10^{8}\times[-4.2293 \quad -0.38977 \quad -0.0396 \quad 0.00907 \quad -0.00358 \quad -0.000479],$$

$$D_{Kf}=10^{7}\times[2.1343 \quad -0.01226 \quad -0.24593].$$

The resulting parameter matrices of the dynamic output feedback controller in entire frequency domain:

$$A_{Ke}=\begin{bmatrix} -20.374 & -1.2329\times10^{7} & 3.6337\times10^{7} & 1.4947\times10^{8} & -1.2458\times10^{9} & 6.8318\times10^{13} \\ -21.988 & 345.37 & -865.65 & -4272.2 & 42471 & -2.3069\times10^{9} \\ 30.146 & -559.14 & 1064.8 & 5771.2 & -55542 & 3.0825\times10^{9} \\ -15.166 & 281.88 & -538.23 & -2917.5 & 27823 & -1.5497\times10^{9} \\ 3.8183 & -67.379 & 141.58 & 724.93 & -7249.3 & 3.9391\times10^{8} \\ -0.00158 & -0.54673 & 15.898 & 28.898 & -16.182 & -1.8669\times10^{5} \end{bmatrix},$$

$$B_{Ke}=10^{9}\times\begin{bmatrix} 0.8031 & -1.8212 & -1.0437 \\ 0.001678 & 0.004893 & 0.01803 \\ 0.026484 & 0.094028 & 0.074239 \\ 0.063187 & 0.022474 & 0.017233 \\ -0.032487 & -0.13933 & 0.082934 \\ -0.28042 & -0.16025 & -0.005605 \end{bmatrix},$$

$$C_{Ke}=[4.7362\times10^{-6} \quad 26.998 \quad -79.575 \quad -327.32 \quad 2728.2 \quad -1.4961\times10^{8}],$$

$$D_{Ke}=[-1855.3 \quad 3993.3 \quad 2285.8].$$

References

[1] Pesterev A, Bergman L, Tan C. A novel approach to the calculation of pothole-induced contact forces in MDOF vehicle models. J Sound Vib 2004;275:127–49.
[2] Thompson A, Davis B. Computation of the rms state variables and control forces in a half-car model with preview active suspension using spectral decomposition methods. J Sound Vib 2005;285:571–83.
[3] Hencey B, Alleyne A. A KYP lemma for LMI regions. IEEE Trans Autom Control 2007;52(10):1926–30.
[4] Kaddissi C, Kenné J. Saad M. Drive by wire control of an electro-hydraulic active suspension a backstepping approach. In: Proceedings of the 2005 IEEE conference on control applications, Toronto, Canada; August 28–31, 2005.
[5] Scherer C, Gahinet P, Chilali M. Multi-objective output-feedback control via LMI optimization. IEEE Trans Autom Control 1997;42(7):896–911.
[6] Gao H, Lam J, Wang C. Multi-objective control of vehicle active suspension systems via load-dependent controllers. J Sound Vib 2006;290:645–75.
[7] Gao H, Zhao Y, Sun W. Input-delayed control of uncertain seat suspension systems with human-body model. IEEE Trans Control Syst Technol 2010;18(3):591–601.
[8] Gao H, Sun W, Shi P. Robust sampled-data H_∞ control for vehicle active suspension systems. IEEE Trans Control Syst Technol 2010;18(1):238–45.
[9] Du H, Lam J, Sze KY. Design of non-fragile H_∞ controller for active vehicle suspensions. J Vib Control 2005;11:225–43.
[10] Du H, Zhang N. H_∞ control of active vehicle suspensions with actuator time delay. J Sound Vib 2007;301:236–52.
[11] Khatibi H, Karimi A, Longchamp R. Fixed-order controller design for polytopic systems using LMIs. IEEE Trans Autom Control 2008;53(1):428–34.
[12] Karimi H, Gao H. Mixed H_2/H_∞ output-feedback control of second-order neutral systems with time-varying state and input delays. ISA Trans 2008;47(3):311–24.
[13] Fialhm I, Balas GJ. Road adaptive active suspension design using linear parameter-varying gain-scheduling. IEEE Trans Control Syst Technol 2002;10(1):43–54.
[14] Marzbanrad J, Ahmadi G, Zohoor H, Hojjat Y. Stochastic optimal preview control of a vehicle suspension. J Sound Vib 2004;275:973–90.
[15] Collado J, Lozano R, Johansson R. On Kalman–Yakubovich–Popov Lemma for stabilizable systems. IEEE Trans Autom Control 2001;46(7):1089–93.
[16] Cheok K, Hu H, Loh N. Discrete-time frequency-shaping parametric LQ control with application to active seat suspension control. IEEE Trans Ind Electron 1989;36(3):383–90.
[17] Wei L, Griffin J. The Prediction of seat transmissibility from measures of seat impedance. J Sound Vib 1998;214(1):121–37.
[18] Zapateiro M, Karimi H, Luo N, et al. Real-time hybrid testing of semiactive control strategies for vibration reduction in a structure with MR damper. Struct Control Health Monit 2010;17(4):427–51.
[19] Yagiz N, Hacioglu Y. Backstepping control of a vehicle with active suspensions. Control Eng Pract 2008;16:1457–67.
[20] Gahinet P, Nemirovskii A, Laub AJ, Chilali M. LMI control toolbox user's guide. Natick, MA: The Math. Works Inc.; 1995.
[21] Apkarian P, Tuan HD, Bernussou J. Continuous-time analysis, eigenstructure assignment, and H_2 synthesis with enhanced Linear Matrix Inequalities (LMI) characterizations. IEEE Trans Autom Control 2001;42(12):1941–6.

[22] Türkay Semiha, Akçay Hüseyin. Aspects of achievable performance for quarter-car active suspensions. J Sound Vib 2008;311:440–60.
[23] Iwasaki T, Hara S. Generalized KYP lemma: unified frequency domain inequalities with design applications. IEEE Trans Autom Control 2005;50(1):41–59.
[24] Iwasaki T, Hara S. Feedback control synthesis of multiple frequency domain specifications via generalized KYP lemma. Int. J. Robust Nonlinear Control 2007;17:415–34.
[25] Sun W, Gao H, Kaynak O. Finite frequency H_∞ control for vehicle active suspension systems. IEEE Trans Control Syst Technol 2010. doi:10.1109/TCST.2010.2042296.
[26] He Y, McPhee J. Multidisciplinary design optimization of mechatronic vehicles with active suspensions. J Sound Vib 2005;283:217–41.
[27] Zhao Y, Sun W, Gao H. Robust control synthesis for seat suspension systems with actuator saturation and time-varying input delay. J Sound Vib 2010;329(21):4335–53.